communications biology

A Nature Portfolio journal

Article

https://doi.org/10.1038/s42003-025-07838-x

Extravascular coagulation regulates haemostasis independently of activated platelet surfaces in an in vivo mouse model

Asuka Sakata[1] ✉, Kohei Tatsumi[1,2], Naoki Matsumoto[1,3], Nigel Mackman[4], Suguru Harada[1,3], Ryohei Kawasaki[1,3], Yukiko Okuyama-Nishida[1,5], Tetsuhiro Soeda[1,3], Keiji Nogami[1,6] & Midori Shima[1]

While the conventional understanding of haemostatic plug formation is that coagulation proceeds efficiently on the surface of activated platelets at the vascular injury site to form a robust haemostatic plug, this understanding does not explain the clinical reality that platelet dysfunction results in a mild bleeding phenotype, whereas coagulation disorders exhibit severe bleeding phenotypes, particularly in deep tissues. Here, we introduce an in vivo imaging method to observe internal bleeding and subsequent haemostatic plug formation in mice and report that haemostatic plug formation after internal bleeding, coagulation occurs primarily outside the blood vessel rather than on platelets. Experiments in mice with impaired platelet surface coagulation, depleted platelets, haemophilia A or reduced tissue factor expression suggest that this extravascular coagulation triggers and regulates haemostatic plug formation. Our discovery of the important role of extravascular coagulation in haemostasis may contribute to refining the treatment of haemostatic abnormalities and advancing antithrombotic therapy.

When bleeding occurs, a haemostatic plug forms to prevent blood loss. Traditionally, it is believed that platelet activation and coagulation occur simultaneously at the injury site, relying on phosphatidylserine (PS) on activated platelets for effective clot formation[1–4]. However, this view does not explain why platelet dysfunction rarely results in severe bleeding, whereas coagulation disorders often do, especially in deep tissues[5].

The ancestors of platelets are believed to be amebocytes found in horseshoe crab haemolymph[6]. These cells release serine proteases, such as prochelicerase C and prochelicerase B[7], which are thought to be the ancestors of coagulation factors. These proteases initiate a cascade of reactions for wound healing[8]. Furthermore, activated amebocytes release serine proteases, antimicrobial peptides, and lectins[9], but unlike human platelets, the cells themselves cannot seal wounds or initiate cascade reactions on their surface[10,11]. Given that coagulation factors are evolutionarily more primitive than platelets are, we hypothesize that coagulation, rather than platelets, is the trigger for haemostasis.

Recent advancements in in vivo imaging techniques have been utilized to examine the process of thrombus formation[12–15]. Two common in vivo imaging techniques for observing thrombus formation are as follows: (1) microscopy after oxidative endothelial injury from chemicals such as ferric chloride[16–18] and (2) microscopy following laser-induced endothelial injury[12,13,15,19–23]. In the oxidative injury model, vascular endothelial desquamation is typically observed after chemical stimulation, although some reports note intact vascular endothelium[24]. Conversely, the conventional laser injury model maintains an intact vascular endothelium, with tissue factor release at the laser site driving thrombus formation[12,19]. Both methods lack bleeding. The presence of a thrombus without bleeding is deemed pathological, leading previous in vivo imaging methods to focus on assessing pathological thromboses rather than haemostasis. In contrast, Bergmeier et al. described a method for inducing external bleeding by applying penetrating laser injury to exposed blood vessels, followed by observation of haemostasis[25,26]. However, to date, no methods have been reported for confirming haemostasis following internal bleeding, which frequently

[1]Medicinal Biology of Thrombosis and Haemostasis, Nara Medical University, 840 Shijo-Cho, Kashihara, Nara, 634-8521, Japan. [2]Advanced Medical Science of Thrombosis and Haemostasis, Nara Medical University, 840 Shijo-Cho, Kashihara, Nara, 634-8521, Japan. [3]Product Research Department, Medical Affairs Division, Chugai Pharmaceutical Co., Ltd., 216 Totsukacho, Totsuka-ku, Yokohama, Kanagawa, 244-8602, Japan. [4]Department of Medicine, Division of Hematology and Oncology, University of North Carolina at Chapel Hill, 116 Manning Drive, Chapel Hill, NC, 27599, USA. [5]Specialty Lifecycle Management Department, Project & Lifecycle Management Unit, Chugai Pharmaceutical Co., Ltd., 1-1 Nihonbashi-Muromachi 2-chome, Nihonbashi Mitsui Tower, Chuo-ku, Tokyo, 103-8324, Japan. [6]Department of Paediatrics, Nara Medical University, 840 Shijo-Cho, Kashihara, Nara, 634-8521, Japan.
✉e-mail: asusaka@naramed-u.ac.jp

occurs in everyday life outside traumatic events. In this study, we developed an in vivo imaging method to observe the early haemostatic response after internal bleeding by disrupting the vascular endothelium via two-photon excitation. Our method confirmed that the haemostatic response remained unaffected in mice with impaired platelet surface coagulation. In contrast, a delayed haemostatic response was observed in mice with low tissue factor expression. These findings indicate that extravascular coagulation acts as the primary trigger for haemostasis during internal bleeding, whereas coagulation on the activated platelet surface is not essential for this process. These novel findings clarify the discrepancy between the traditional understanding of haemostasis and clinical observations regarding platelet dysfunction. These findings could also contribute to improved management of haemostatic abnormalities and to advances in antithrombotic therapy.

Results

Fibrin is formed outside blood vessels

We developed an in vivo imaging method to observe bleeding and haemostatic plug formation in veins and arteries, with a focus on platelets and coagulation after internal bleeding. In C57BL/6J (wild-type) mice, we observed that venous and arterial haemostatic plugs contained platelet aggregates inside the vessel, fibrin in platelet-free areas outside the vessel, and coexisting platelet and fibrin clots at the boundaries (Fig. 1a, b).

Haemostasis after arterial internal bleeding was completed by cessation of plasma leakage following cessation of blood cell leakage

In our experiments, venous internal bleeding included plasma leakage, identified by fluorescent dextran leakage, with minimal blood cell leakage. In contrast, arterial internal bleeding resulted in both blood cell and plasma leakage, with red blood cells visible as black silhouettes (Fig. 1a, b). To confirm how blood cell and plasma leakage ceases during haemostasis after arterial internal bleeding, we analysed images of significant vascular damage (25–40 mm) that allowed clear observation of blood cell leakage. Consequently, haemostasis was achieved first with the cessation of blood cell leakage, followed by the cessation of plasma leakage. Low plasma leakage results in slight fluctuations in the dextran signal, making it difficult to determine when leakage stops. However, during blood cell leakage, clear extravascular leakage of fluorescent dextran was observed in all mice.

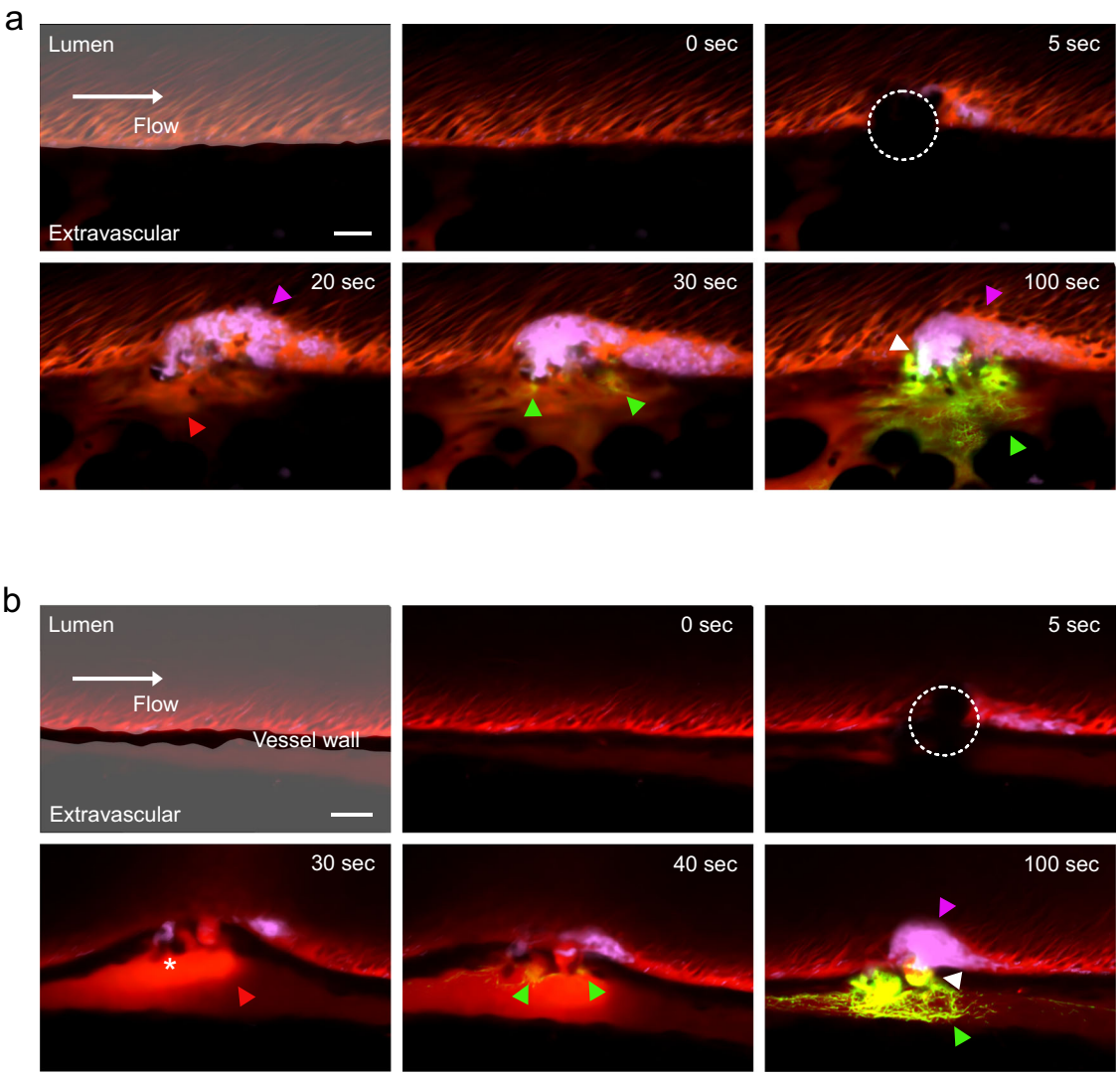

Fig. 1 | Fibrin, a component of haemostatic plugs, is formed outside blood vessels. Representative images of haemostatic plug formation after venous (**a**) and arterial (**b**) internal bleeding. The mice were intravenously injected with dextran-rhodamine B, Alexa Fluor 488-conjugated fibrinogen and the platelet imaging antibody X649 prior to observation. After two-photon excitation injury (circle of dots), platelet aggregate formation in the lumen (magenta triangle) and extravascular plasma leakage (red triangle) were observed. After arterial internal bleeding, red blood cell leakage was observed (white asterisk). Fibrin is formed in the extravascular area (green triangle). The haemostatic plug consisted of a platelet aggregate in the lumen, extravascular fibrin, and platelets and fibrin at the boundary of the lumen and extravascular space (white triangle). Scale bar = 20 μm. Green: fibrin/fibrinogen. Magenta: platelets. Red: plasma.

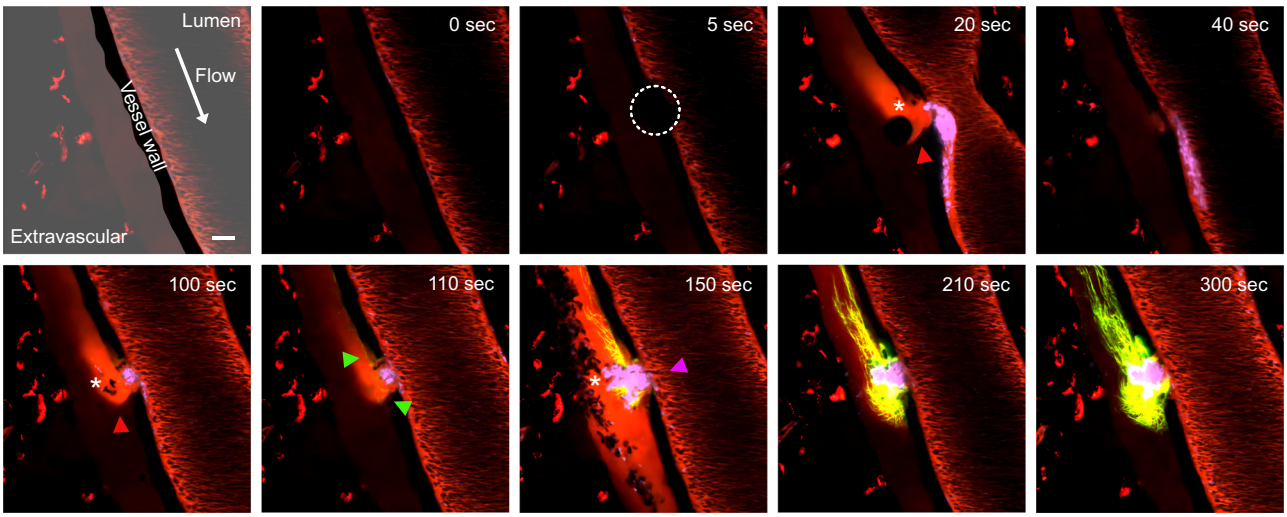

Fig. 2 | Haemostasis was achieved by the cessation of plasma leakage following the cessation of blood cell leakage. Representative images of haemostatic plug formation after arterial internal bleeding from a large injury. The mice were intravenously injected with dextran-rhodamine B, Alexa Fluor 488-conjugated fibrinogen, and the platelet imaging antibody X649 prior to observation. After two-photon excitation injury (circle of dots), extravascular plasma leakage (red triangle) and red blood cell leakage were observed (white asterisk). Vasoconstriction temporarily reduced blood leakage, but it resumed when vasoconstriction was released. Fibrin begins to form in slow-flowing areas of the extravascular space (green triangle). Exacerbated blood cell leakage stopped when platelets clogged the site of vessel rupture (magenta triangle). Fibrin formation proceeded in the area of slowed flow caused by platelet blockage, resulting in the cessation of plasma leakage. Scale bar = 20 μm. Green: fibrin/fibrinogen. Magenta: platelets. Red: plasma.

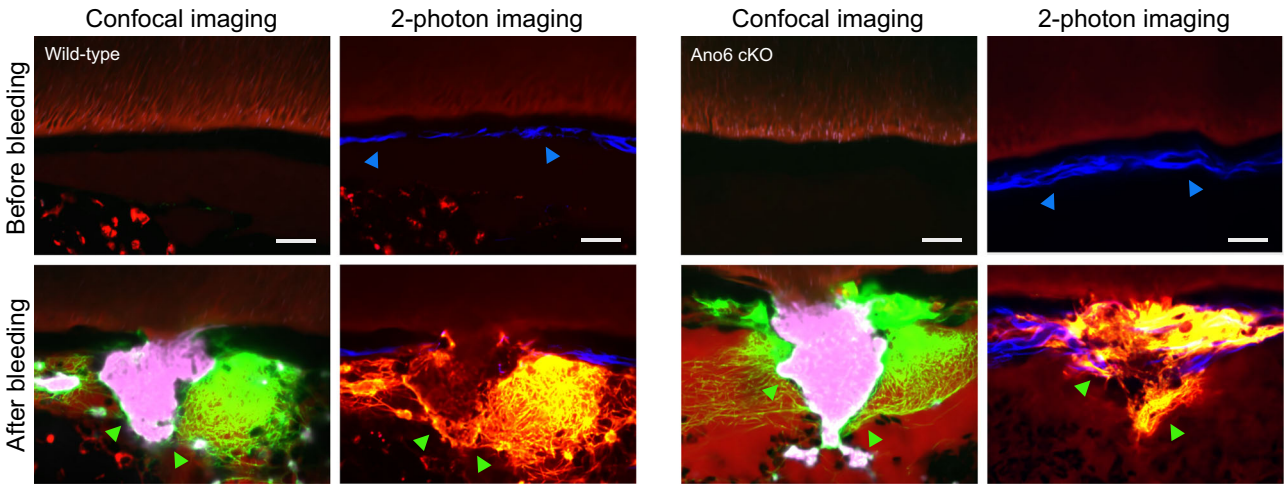

Fig. 3 | Platelets are trapped by extravascular fibrin where collagen is damaged. Representative images of haemostatic plugs after large arterial injury. The mice were intravenously injected with dextran-rhodamine B, Alexa Fluor 488-conjugated fibrinogen, and the platelet imaging antibody X649 prior to observation. Vessel observation before the arterial injury and after haemostatic plug formation via two-photon imaging revealed collagen (blue triangle) and platelets attached to the fibrin network (green triangle), where collagen ruptured. Similar findings were observed in Ano6 cKO mice with impaired platelet coagulation. Scale bar = 20 μm. In the confocal images, green indicates fibrin/fibrinogen, magenta indicates platelets, and red indicates plasma. In two-photon images, yellow-green indicates fibrin/fibrinogen, red indicates plasma, and blue indicates collagen.

Although blood cell leakage recurred, it ceased when platelets clog the vascular injury site (Fig. 2).

To investigate platelet entrapment outside the vessel, we observed bleeding sites in wild-type mice via two-photon imaging, which is known for its ability to visualize collagen[27]. We observed that leaking platelets were attached to fibrin where collagen was disrupted. Similar findings were noted in platelet-specific anoctamin-6 (TMEM16F) knockout (Ano6 cKO) mice, a murine model of Scott's syndrome characterized by impaired expression of PS on platelets[28]. This finding indicated that fibrin entrapped leaked platelets independently of platelet activation (Fig. 3).

Irreversible platelet activation was not observed in the early phase of haemostatic plug formation

We then investigated the activation status of platelets in haemostasis by examining CD62P, a marker of irreversibly activated platelets. While CD62P was detected in platelets that clog the liver vasculature after intravenous thrombin injection (positive control, Fig. 4a), it was not detected in the in vivo bleeding/haemostasis model, in accordance with our hypothesis (Fig. 4b). These findings suggest that platelets exhibit limited activation during the early phase of haemostatic plug formation, with coagulation predominantly occurring outside the vessel.

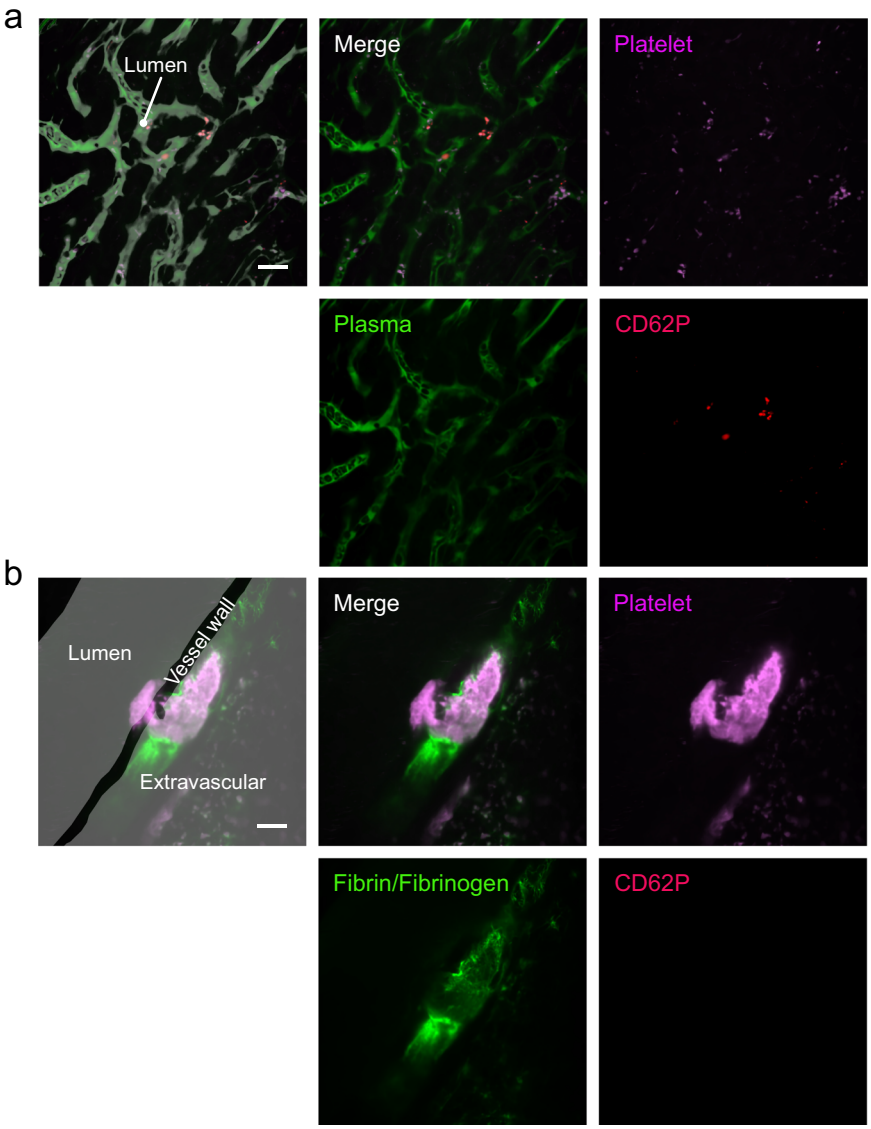

Fig. 4 | Irreversible platelet activation does not occur in early haemostatic plugs. Representative images of platelets that clog the liver vasculature after systemic thrombin injection (**a**) and haemostatic plugs that formed after large arterial injury (**b**). For arterial haemostatic plug observation, the mice were injected with Alexa Fluor 488-conjugated fibrinogen, PE-conjugated rat anti-mouse CD62P antibody, and platelet imaging antibody X649 prior to observation. For platelet observation after thrombin injection, the mice were injected with FITC-dextran, PE-conjugated rat anti-mouse CD62P antibody, and X649 antibody prior to observation. CD62P expression was detected on platelets that clog the liver vasculature (**a**) but was not detected in the in vivo internal bleeding/haemostasis model (**b**). Scale bar = 20 μm. Green: fibrin/fibrinogen. Magenta: platelets. Red: plasma.

Quantitative analysis of haemostatic plug formation in wild-type, Ano6 cKO, platelet-depleted, FVIII KO, and low-tissue-factor mice

To investigate the role of platelets and coagulation in haemostatic plug formation, we analysed images from wild-type, platelet-depleted (administered antibodies for platelet depletion with platelet counts of approximately 3% of the predose level), and three genetically modified mouse strains, Ano6 cKO; coagulation factor VIII-deficient (FVIII KO), which represent severe haemophilia A; and low-tissue-factor-expressing (L-TF) mice, which are indicative of an impaired extrinsic coagulation pathway, were used. We focused on lesions within specific vascular injury ranges—25–40 μm for veins (wild-type, $n = 6$ lesions of 5 animals; Ano6 cKO, $n = 5$ lesions of 5 animals; platelet-depleted, $n = 5$ lesions of 5 animals; FVIII KO, $n = 6$ lesions of 4 animals; and L-TF mice, $n = 16$ lesions of 4 animals) and 10–25 μm for arteries (wild-type, $n = 6$ lesions of 6 animals; Ano6 cKO, $n = 7$ lesions of 6 animals; platelet-depleted, $n = 5$ lesions of 5 animals; FVIII KO, $n = 5$ lesions of 5 animals; and L-TF mice, $n = 6$ lesions of 6 animals)—ensuring accuracy in our evaluations. Representative images and movies are shown in Figs. 5, 6, and Supplementary Movies 1–10. Figures 7a, 8a, Supplementary Figs. 1 and 2 show time-series data obtained from individual mice, while Figs. 7b–f and 8b–h present extracted data related to platelet aggregates, fibrin, and bleeding.

Extravascular coagulation is important for stable platelet aggregate formation

Statistical analysis of platelet aggregates formed after venous internal bleeding revealed a significantly lower peak height in L-TF mice than in wild-type ($p = 0.0024$), Ano6 cKO ($p = 0.0005$), and FVIII KO mice ($p = 0.0012$) (Fig. 7b). A comparison of aggregates formed between 0–120 s (early-stage) and between 120–300 s (late-stage) revealed a lower peak height in the late-stage for both FVIII KO ($p = 0.031$) and L-TF mice ($p < 0.0001$) (Fig. 7c). After arterial bleeding, peak heights did not differ among mouse types (Fig. 8b), except in platelet-depleted mice. When comparing early- and late-stage platelet aggregates, the peak height tended to be lower in the late-stage in FVIII KO and L-TF mice ($p = 0.063$) (Fig. 8c). These findings suggest the importance of extravascular coagulation in venous and arterial platelet aggregates.

Extravascular coagulation proceeds independently of the activated platelet surface

As bleeding progresses, the formation of extravascular fibrin increases, except in L-TF mice. Thus, to assess coagulation efficiency, we quantified fibrin formation acceleration rather than the total fibrin area. After venous internal bleeding, FVIII KO mice exhibited significantly lower acceleration compared to wild-type ($p = 0.0025$), Ano6 cKO ($p = 0.044$), and platelet-depleted mice ($p = 0.020$) (Fig. 7d). No significant difference was observed

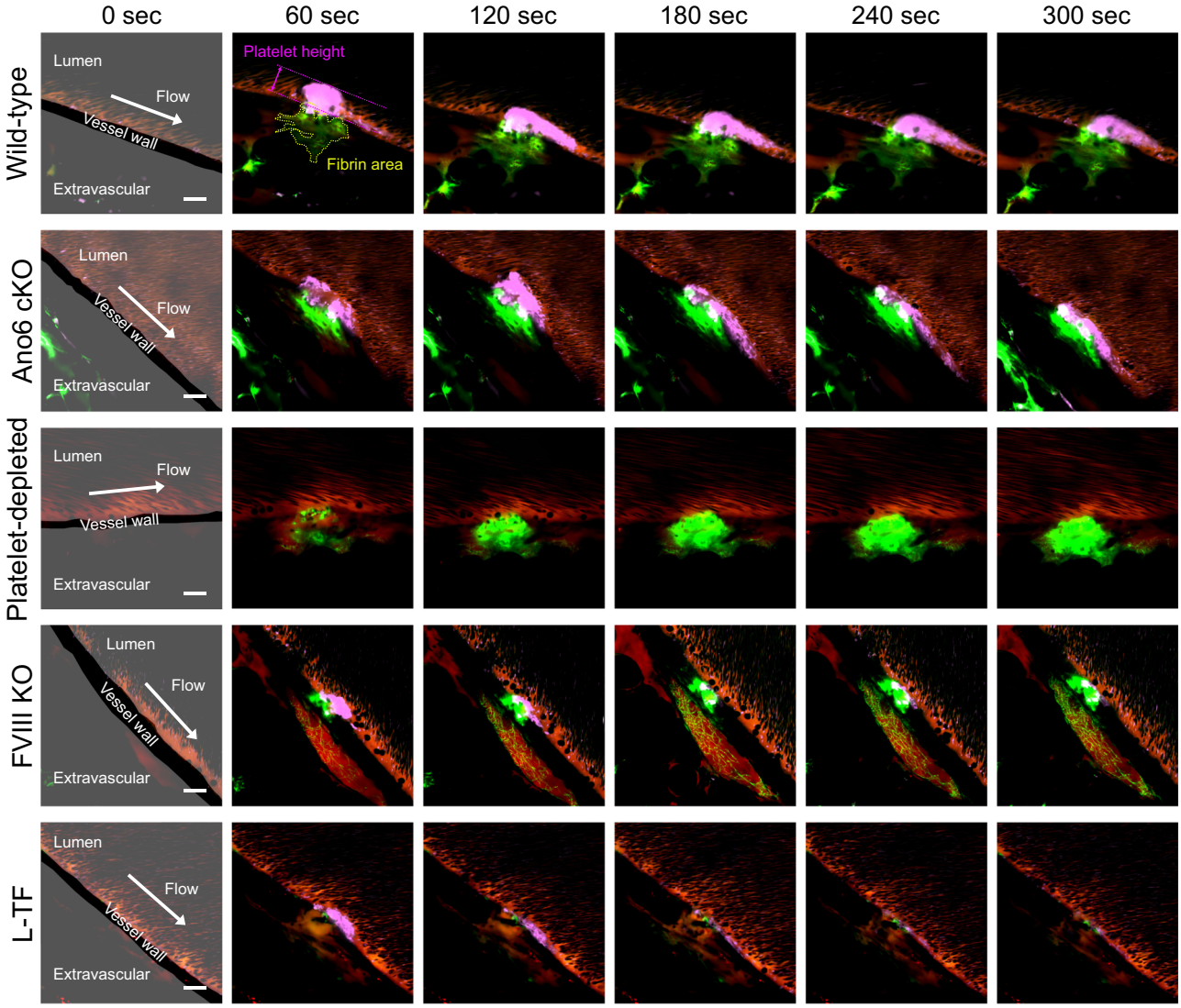

Fig. 5 | Haemostatic plug formation after venous internal bleeding in wild-type, Ano6 cKO, platelet-depleted, FVIII KO, and L-TF mice. Representative images of haemostatic plug formation after venous internal bleeding in wild-type, Ano6 cKO, platelet-depleted, FVIII KO, and L-TF mice. The mice were intravenously injected with dextran-rhodamine B, Alexa Fluor 488-conjugated fibrinogen, and the platelet imaging antibody X649 prior to observation. Scale bar = 20 μm. Green: fibrin/fibrinogen. Magenta: platelets. Red: plasma.

between wild-type and Ano6 cKO mice ($p = 0.30$). Following arterial internal bleeding, while the acceleration in platelet-depleted mice tended to be greater than that in FVIII KO mice ($p = 0.098$), no significant differences were found among the groups (Fig. 8d). These findings suggest that extravascular fibrin formation occurs independently of activated platelet surfaces in both veins and arteries.

Extravascular fibrin formation is important for the cessation of both blood cell and plasma leakage

Under our experimental conditions, minimal blood cell leakage occurred after venous injury. In terms of arterial internal bleeding, the time from bleeding onset to cessation of blood cell leakage was significantly longer in platelet-depleted and L-TF mice than in wild-type and Ano6 cKO mice (wild-type vs. platelet-depleted, $p = 0.014$; wild-type vs. L-TF, $p = 0.0045$; Ano6 cKO vs. platelet-depleted, $p = 0.0064$; and Ano6 cKO vs. L-TF, $p = 0.0018$) (Fig. 8g). Platelet extravasation revealed a significantly greater distance from the vascular endothelium to extravasated platelets in L-TF mice than in wild-type ($p = 0.0054$) and Ano6 cKO mice ($p = 0.033$) (Fig. 8h). Additionally, plasma leakage from internal venous bleeding was significantly greater in L-TF mice than in wild-type ($p < 0.0001$), FVIII KO ($p = 0.0023$), and Ano6 cKO mice ($p = 0.0005$) (Fig. 7f), whereas arterial internal bleeding was significantly greater in L-TF mice than in wild-type mice ($p = 0.027$), with a trend towards platelet-depleted mice ($p = 0.064$) (Fig. 8f). These findings highlight the importance of extravascular fibrin formation in achieving complete haemostasis.

Discussion

Haemostatic plug formation is traditionally thought to involve efficient coagulation on the surface of activated platelets[1–4], suggesting that platelet dysfunction should lead to severe bleeding. However, in the clinic, platelet dysfunction disorders, such as thrombasthenia or Scott syndrome, cause minimal bleeding, whereas coagulation disorders, such as haemophilia, lead to severe joint or muscle bleeding[5]. The aim of this study was to elucidate the sites and roles of coagulation in haemostatic plug formation through in vivo imaging of internal bleeding. These findings suggest that extravascular coagulation, rather than coagulation on activated platelets, is crucial in initiating and regulating haemostasis following internal bleeding.

In vascular injury induced by conventional one-photon excitation, damage occurs not only in the targeted area but also in the superficial and deep surrounding regions. In contrast, our method of inflicting vascular

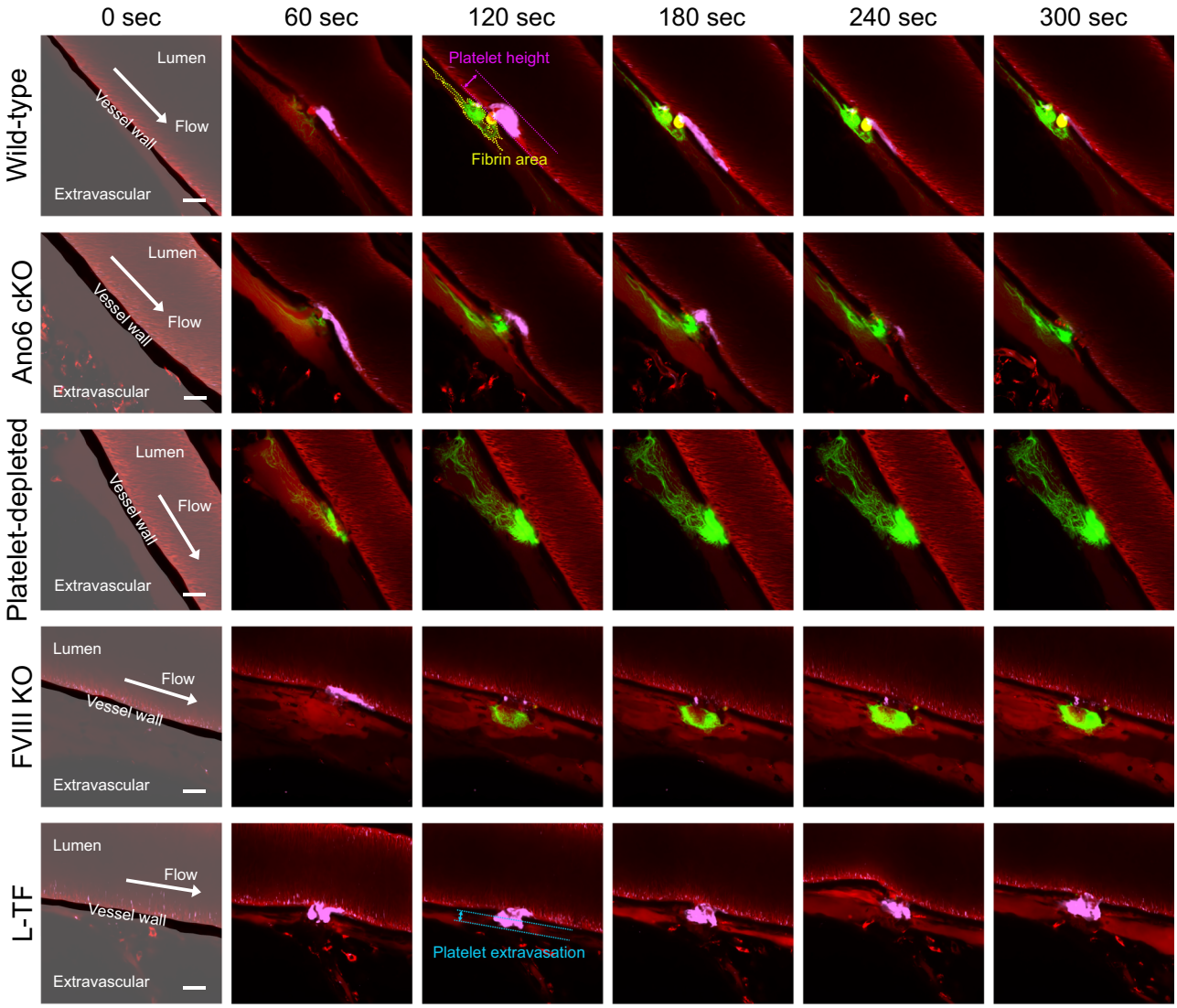

Fig. 6 | Haemostatic plug formation after arterial internal bleeding in wild-type, Ano6 cKO, platelet-depleted, FVIII KO, and L-TF mice. Representative images of haemostatic plug formation after arterial internal bleeding in wild-type, Ano6 cKO, platelet-depleted, FVIII KO, and L-TF mice. The mice were intravenously injected with dextran-rhodamine B, Alexa Fluor 488-conjugated fibrinogen, and the platelet imaging antibody X649 prior to observation. Scale bar = 20 μm. Green: fibrin/fibrinogen. Magenta: platelets. Red: plasma.

injury with two-photon excitation can induce localized damage at the targeted depth without injuring the areas traversed by the laser. In this model, blood leaks from the vessel into the surrounding undamaged tissue. In the external bleeding model of Bergmeier et al., haemostatic plugs are observed exclusively within the intravascular space and at the boundary between intravascular and extravascular regions[25,26]. In contrast, in our internal bleeding model, haemostatic plugs are more widely distributed, extending from the intravascular area into the extravascular space. To determine whether the haemostatic plug observed in our model, which is composed of extravascular fibrin, intravascular platelet aggregate, and a clot consisting of both platelets and fibrin at the vascular boundary (Fig. 1a, b), is specific to our model, we punctured the mouse medial saphenous vein or artery with a 30 G needle and applied compression to halt bleeding. The resulting plug, containing extravascular fibrin and intravascular platelet aggregates, was similar to our model (Supplementary Fig. 3). Thus, we conclude that the plugs observed in our model resemble those resulting from vascular injury in mammals.

A clot of platelets and fibrin formed at the intra/extravascular boundary following the formation of extravascular fibrin, which was similarly observed in Ano6 cKO mice (Fig. 5). Extravascular fibrin formed even in the platelet-depleted and Ano6 cKO mice (Figs. 5 and 6). These findings indicate that coagulation on the surface of platelets plays a minor role in fibrin formation in our internal bleeding/haemostasis model. Notably, platelets involved in early haemostasis did not express CD62P, a marker of irreversibly activated platelets that serve as a site of coagulation (Fig. 4), which aligns with prior findings of no PS exposure on platelets even up to 30 min after bleeding[29]. In contrast, Bergmeier et al. reported that fibrin formed primarily on platelets with PS exposure in an external bleeding model[26]. This difference may stem from the fact that, in our internal bleeding model, blood leakage into an enclosed space rich in tissue factor allows coagulation to proceed even in the absence of activated platelets. Sufficient thrombin generation occurs not only on activated platelets but also on tissue factor-bearing cells[30], and extravascular cells support the formation of a dense, fibrinolysis-resistant fibrin network[31]. Our findings and previous reports suggest that early after internal bleeding, platelet activation is limited, preventing coagulation within blood vessels while allowing rapid fibrin formation outside vessels. This mechanism may reduce the risk of pathological thrombosis and prevent exsanguination.

In our study, venous internal bleeding primarily caused plasma leakage with minimal blood cell leakage, whereas arterial internal bleeding involved

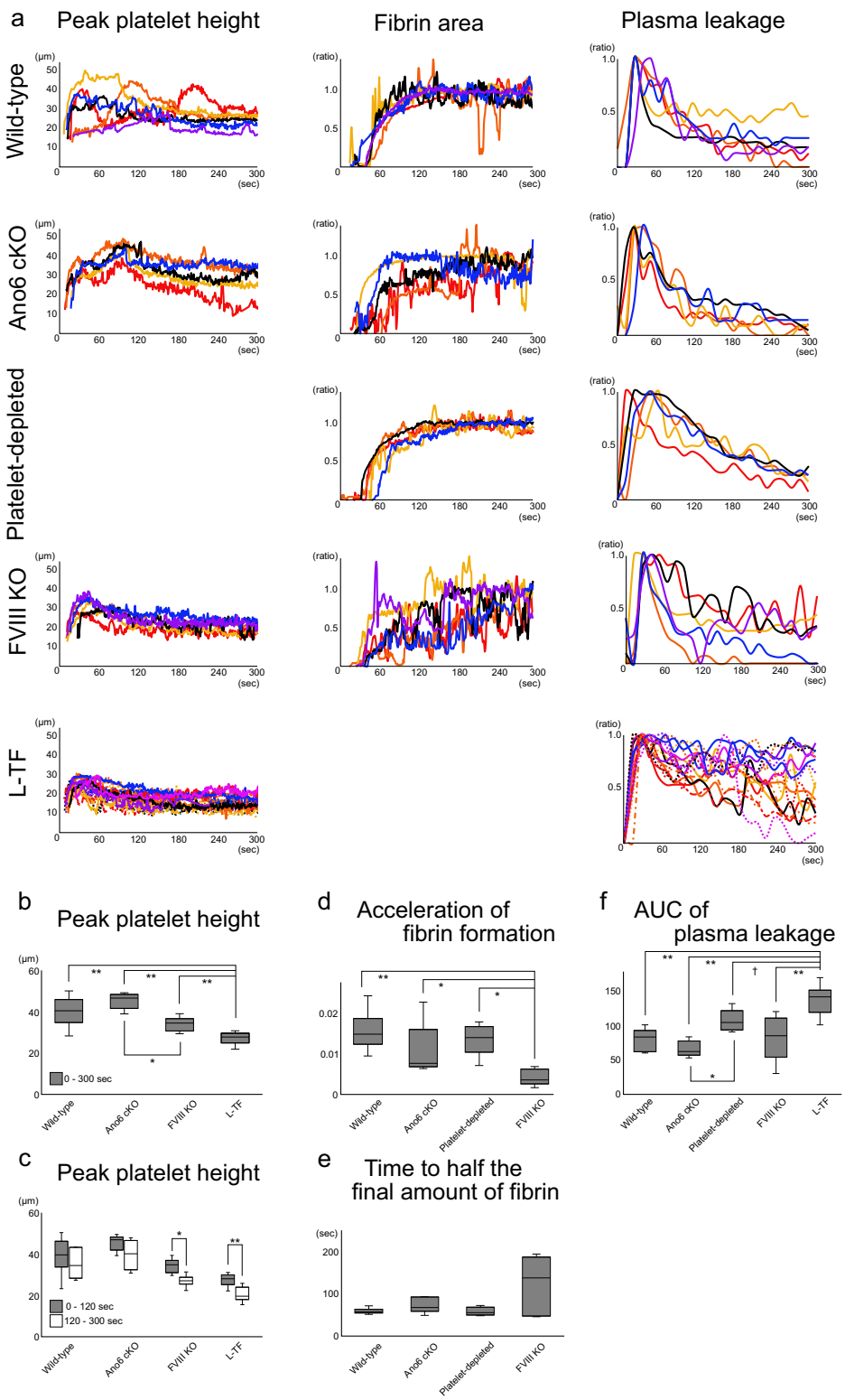

Fig. 7 | Extravascular coagulation is important for platelet aggregate formation and the cessation of plasma leakage after venous internal bleeding. Measurements of platelet aggregates, fibrin, and plasma leakage were taken from experimental mice (**a**) (wild-type, $n = 6$ lesions from 5 animals; Ano6 cKO, $n = 5$ lesions from 5 animals; platelet-depleted, $n = 5$ lesions from 5 animals; FVIII KO, $n = 6$ lesions from 4 animals; and L-TF mice, $n = 16$ lesions from 4 animals). Platelet aggregates were assessed by height from the vascular endothelium. Fibrin was quantified as the ratio of the fibrin area over time, normalized to the end of the observation period. Plasma leakage was expressed relative to the maximum signal outside the vessel. Box-and-whisker plot of the peak platelet aggregate height (**b**). Peak platelet aggregate height at 0–120 and 120–300 s (**c**). The increase in the fibrin area accelerated, as indicated by the ratio (**d**). Time required for the fibrin area to reach half the area at the end of observation (**e**). Area under the curve (AUC) of plasma leakage (**f**). *<0.05, **<0.01. **c** Wilcoxon signed-rank test; **b**, **d**–**f** Steel–Dwass test and Monte Carlo simulation.

leakage of both. During arterial internal bleeding, haemostasis occurred first with cessation of blood cell leakage, followed by cessation of plasma leakage (Figs. 1b, 2, 8a, g). L-TF and platelet-depleted mice had a significantly longer time to cease blood cell leakage (Fig. 8g). Although plasma leakage did not differ between wild-type and Ano6 cKO mice, it increased in L-TF mice with venous bleeding (Fig. 7f) and in L-TF and platelet-depleted mice with arterial bleeding (Fig. 8f). These findings highlight the critical role of extravascular coagulation in haemostasis in both veins and arteries, with platelets potentially contributing additional roles in arterial haemostasis other than PS exposure. While fibrin formation rates were not significantly different among the wild-type, Ano6 cKO, and platelet-depleted mice (Figs. 7d and 8d), the platelet-depleted mice spent more time reaching half the final fibrin amount during arterial internal bleeding (Fig. 8e), indicating that platelets help regulate blood flow at injury sites, promoting effective coagulation.

To elucidate the role of extravascular coagulation in platelet aggregate formation (Fig. 1a, b), we compared the heights of platelet aggregates among various mouse groups. In veins, L-TF mice presented significantly lower

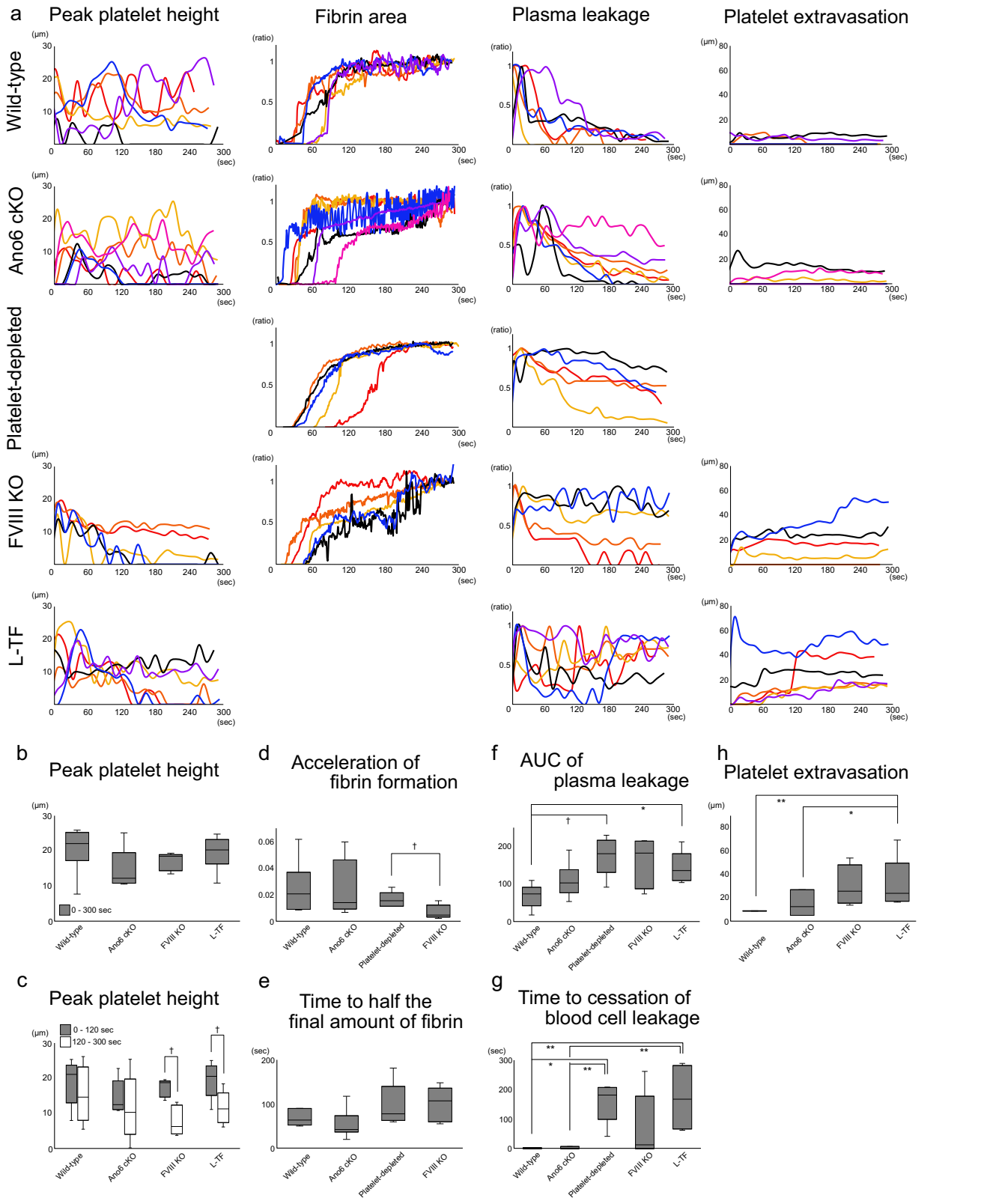

maximum platelet aggregate heights (Fig. 7b), emphasizing the role of extravascular coagulation through the TF-triggered extrinsic pathway. In the arteries, the maximum platelet aggregate height did not significantly differ among the wild-type, Ano6 cKO, FVIII KO, and L-TF mice (Fig. 8b). However, when comparing early-stage (0–120 s) and late-stage (120–300 s) platelet aggregates in both veins and arteries, FVIII KO and L-TF mice exhibited lower late-stage platelet aggregates (Figs. 7c and 8c). These findings suggest that in veins, platelet aggregate formation involves TF-triggered coagulation from the early-stage, whereas in arteries, coagulation becomes significant in the late-stage, with early activation driven by shear stress[32,33]. Platelets are regulated by both shear stress and extravascular coagulation. Extravascular thrombin activates platelets via PAR1 receptors[34] (and PAR3

Fig. 8 | Extravascular coagulation is important for the formation of platelet aggregates and the cessation of blood cell and plasma leakage after arterial internal bleeding. Measurements of platelet aggregates, fibrin, and plasma leakage were taken from experimental mice (**a**) (wild-type, $n = 6$ lesions of 6 animals; Ano6 cKO, $n = 7$ lesions of 6 animals; platelet-depleted, $n = 5$ lesions of 5 animals; FVIII KO, $n = 5$ lesions of 5 animals; and L-TF mice, $n = 6$ lesions of 6 animals). Platelet aggregates were assessed by height from the vascular endothelium. Fibrin was quantified as the ratio of the fibrin area over time, normalized to the end of the observation period. Plasma leakage was expressed relative to the maximum signal outside the vessel. Box-and-whisker plot of the peak platelet aggregate height (**b**). Peak platelet aggregate height at 0–120 and 120–300 s (**c**). The increase in the fibrin area accelerated, as indicated by the ratio (**d**). Time required for the fibrin area to reach half the area at the end of observation (**e**). Area under the curve (AUC) of plasma leakage (**f**). The time from the start of bleeding to the cessation of blood cell leakage (**g**). The extent of platelet aggregate extrusion from the vessel was evaluated by measuring the distance from the vessel wall to the platelets, as shown in (**h**). †<0.1, *<0.05, **<0.01. **c** Wilcoxon signed-rank test; **b**, **d**–**h** Steel–Dwass test and Monte Carlo simulation.

and PAR4 receptors in mice[35]), whereas thrombin and factor Xa activate the vascular endothelium via PAR1 and PAR2[36]. This dual regulation may explain the reduced platelet aggregate height in mice with impaired extravascular coagulation. The mechanism by which extravascular coagulation influences haemostatic plug formation, including intravascular platelet aggregate formation, seems reasonable, as it helps prevent excessive thrombus formation once haemostasis is achieved.

Limitations

This study has several limitations. First, the vascular injury was observed under restricted conditions, limiting our understanding of how it affects haemostatic plug and thrombus formation in different vessels or different extents of damage. Second, during arterial internal bleeding, vasoconstriction causes discrepancies in the timing of bleeding exacerbation among mice, highlighting the need to understand its role in haemostatic plug formation. Third, we injected human fibrinogen conjugated with a fluorescent dye for in vivo observation, which means that we may have underestimated fibrin thrombi since we did not observe mouse fibrin clots. Finally, the anaesthetic urethane may influence the results by inducing sympathetic nervous system excitement, and its use poses challenges for replicating study conditions, as it is no longer recommended in animal experiments. The results of the evaluation of the effects of anaesthetic urethane compared with alternative anaesthetics (a combination of medetomidine, butorphanol and midazolam) are given in the Supplementary Information.

Conclusion

Our understanding of the impact of extravascular coagulation on haemostasis after internal bleeding is shown in Fig. 9. Our findings, together with those of previous reports[25,26], suggest that the platelet surface is the site of coagulation in external bleeding and that the extravascular tissue is the site of coagulation in internal bleeding, which may explain the phenotype of platelet dysfunction, with frequent nasal and gum bleeding[5] (external bleeding) and coagulation disorders with frequent deep tissue bleeding[5] (internal bleeding). These insights could inform clinical treatment strategies, such as administering coagulation factors with plasma transfusion in severe trauma, aligning with findings from the PAMPer[37] and COMBAT[38] clinical trials that highlight benefits in emergency settings. While many clotting factor replacements and mimetics are designed for prolonged retention in the bloodstream, optimizing their concentration outside the vasculature could enable drug development that enhances haemostasis while reducing thrombosis risk. Additionally, if fibrinolytic drugs used for thrombosis treatment could be engineered to remain inactive outside the vascular system, it may become possible to manage thrombosis more safely.

In conclusion, we demonstrated the critical role of extravascular coagulation in the formation of haemostatic plugs following internal bleeding via in vivo imaging. These findings have the potential to enhance our understanding of bleeding symptoms in clinical settings and contribute to the development of more effective and safer therapeutic drugs. Furthermore, this research method proved to be a valuable tool for evaluating such drugs.

Methods

Mice

Male C57BL/6J (wild-type) mice, FVIII-deficient (FVIII KO) mice (B6;129S-F8tm1Kaz/J)[39] and low-TF-expressing (L-TF) mice[40], all with a matching genetic background, were used. These mice were aged 8–13 weeks and weighed 22–25 g. Platelet-specific anoctamin-6 (TMEM16F) knockout (Ano6 cKO) mice were generated by crossing anoctamin-6 flox/flox (B6.Cg-Ano6tm1.1Naga)[41] and Pf4-iCre transgenic mice[42]. Wild-type mice received an intravenous injection of 2 mg/kg R300 antibody (Emfret Analytics GmbH & Co., KG, Würzburg, Germany)[43] to obtain platelet-depleted mice. Wild-type mice were purchased from Japan SLC, Inc. (Shizuoka, Japan). FVIII KO and Pf4-iCre mice were obtained from The Jackson Laboratory (Maine, USA). Anoctamin-6 flox/flox mice were provided by Riken BRC (Ibaraki, Japan). L-TF mice were provided by Prof. Nigel Mackman (University of North Carolina at Chapel Hill). Mice obtained from other facilities were housed in the Institute of Experimental Animal Science at Nara Medical University for at least one week to allow for acclimatisation. The mice were kept under controlled conditions (20–26 °C, 40–60% humidity) with a 12-h light/dark cycle and had ad libitum access to food and water. Anaesthesia was induced via intraperitoneal injection of urethane (1.5 mg/kg). After observation, the mice were euthanized by cervical dislocation. The depth of anaesthesia was confirmed by the hindlimb retraction reflex and the abdominal skin pain reflex. All animal experiments were approved by the Institutional Animal Care and Use Committee and strictly followed the guidelines for animal experiments of Nara Medical University (Permit Nos. 13320, 13323, and 13387).

In vivo imaging of internal bleeding and haemostatic plug formation after two-photon excitation injury

An A1R-MP microscope (Nikon, Japan) was used for visual analysis of bleeding and haemostatic plug formation in the testicular artery and medial saphenous vein. After sufficient anaesthesia was achieved, two small incisions were made in the median abdomen and medial thigh to observe blood vessels on the surface of the testis and under the skin of the thigh. Mice were injected via the jugular vein with dextran-rhodamine B (MW 70 kDa) (Merck KGaA, Darmstadt, Germany) (40 μg/g body weight), Alexa Fluor 488-conjugated fibrinogen (Thermo Fisher, Massachusetts, USA) (30 μg/g body weight) and X649 antibody (Emfret) (0.1 μg/g body weight), which labels platelets in mice without affecting their function. The mice were placed on a heated stage (Tokaihit, Shizuoka, Japan), and transverse sections of the testicular arteries and medial saphenous veins were visualized via confocal imaging (lens: Nikon Apo LWD ×40/1.15 WI λS, scanner zoom: 1.5×). The endothelium was cauterized by two-photon excitation with a pulsed laser at 800 nm (laser power: ~2064 mW) (laser source: COHERENT Verdi 18 W) (Coherent, Pennsylvania, U.S.A.), with an injury time of 0.8–1.6 s. Laser irradiation was stopped immediately after bleeding was obtained, and the irradiation area was 40 μm in diameter. After vascular injury, extravascular collagen was observed via two-photon microscopy at 930 nm in the same area. The total observation time was 5 min.

In vivo imaging of platelet activation

After the appropriate depth of anaesthesia was achieved, small incisions were made to observe the testis, and Alexa Fluor 488-conjugated fibrinogen, 25 μL of PE-conjugated rat anti-mouse CD62P antibody (Emfret), and X649 antibody were injected intravenously. Platelets involved in haemostasis were then observed in the testicular artery of wild-type mice via microscopy following two-photon excitation injury. In the positive control, small incisions were made in the median upper abdomen to observe the liver after it reached the appropriate depth of anaesthesia. FITC-dextran (MW 70 kDa) (Merck KGaA) (8 μg per g body weight), PE-conjugated rat anti-mouse

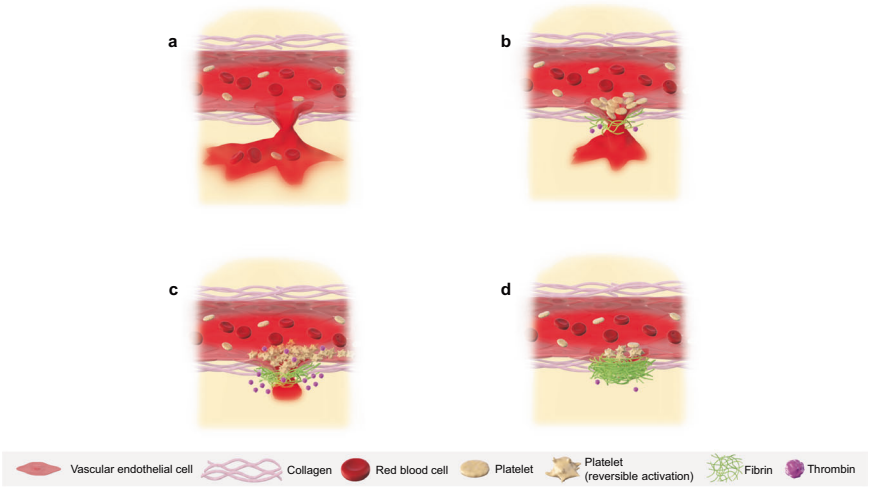

Fig. 9 | Extravascular coagulation triggers and regulates haemostasis. When vascular continuity is lost, blood cells and plasma leak out of the vessels (**a**). Extravascular fibrin and platelets captured by fibrin inhibit blood cell and plasma leakage (**b**). Coagulation proceeds extravascularly, and the generated thrombin accelerates extravascular fibrin formation and activates platelets in the lumen (**c**). As extravascular fibrin grows, plasma leakage ceases, resulting in complete haemostasis (**d**).

CD62P antibody, X649 antibody, and 1 U per body thrombin (Fuji Pharma Co., Ltd., Tokyo, Japan) were injected intravenously, and platelets were observed in the liver vasculature via microscopy.

Image analysis

For quantitative analysis of bleeding and fibrin/platelet aggregate formation, the acquired sequential images were first denoised with NIS-Elements Advanced Research (AR) version 5.21.00 (Nikon). Images with vascular damage areas of 25–40 μm for venous bleeding and 10–25 μm for arterial bleeding were then extracted. Platelet, fibrin, and plasma signals were quantified via NIS-Elements AR. The height of adhered platelet aggregates from the endothelial end to the luminal end, defined as the platelet height, was measured (Figs. 7 and 8). The protrusion of platelet aggregates outside the vessel was assessed by their length beyond the vascular endothelium (Fig. 8). Fibrin was quantified by the area of fibrin formed (Figs. 7 and 8), which was determined by the stronger signals compared with circulated blood, and bleeding was measured by the leaked blood cells and the signal of leaked plasma. The data were analysed via Microsoft® Excel for Mac version 16.79.1. The maximum platelet height was defined as the peak height.

For bleeding analysis, the maximum intensity of the leaked plasma signal was normalized to 1. In veins, the area under the curve (AUC) of the leaked plasma signal was calculated from 1 to 181 s; in arteries, it was calculated from the time of a 0.4 bleeding signal to 246 s. The fibrin signals in the veins were normalized to a minimum of 0 and a convergence value of 1. For FVIII KO mice, a quadratic fitting curve was generated from values above 0. Other strains' signals from 0 to 120 s were used to create quadratic fitting curves. The slope of the tangent line for a signal of 0.5 was calculated for these curves. In arteries, a quadratic fitting curve was created from fibrin signals ranging from 0.2 to 0.8, and the slope for 0.5 was similarly calculated. The time for blood cells to stop leaking was confirmed via video.

Statistics and Reproducibility

Statistical analyses were conducted via RStudio version 2023.12.0 + 369, with R version 4.3.2 (R Foundation for Statistical Computing, Vienna, Austria). The Wilcoxon signed-rank test was used to compare matched pairs via the 'exactRankTests' package (version 0.8-35), whereas the Steel–Dwass test with the Monte Carlo method for three or more independent groups was performed via the 'NSM3' package (version 1.18). P values < 0.05 indicated statistical significance.

Data availability

Source data underlying the graphs presented in the main figures are available in Supplementary Data 1 and 2. Other datasets including R scripts used in this study, are available from the corresponding author upon request.

Code availability

In this study, the researchers did not generate any new custom code.

Received: 29 August 2024; Accepted: 26 February 2025;
Published online: 08 March 2025

References

1. Hoffman, M. Remodeling the blood coagulation cascade. *J. Thromb. Thrombolysis* **16**, 17–20 (2003).
2. Dahlbäck, B. Blood coagulation. *Lancet* **355**, 1627–1632 (2000).
3. Kjalke, M. et al. Active site-inactivated factors VIIa, Xa, and IXa inhibit individual steps in a cell-based model of tissue factor-initiated coagulation. *Thromb. Haemost.* **80**, 578–584 (1998).
4. Oliver, J. A., Monroe, D. M., Roberts, H. R. & Hoffman, M. Thrombin activates factor XI on activated platelets in the absence of factor XII. *Arterioscler. Thromb. Vasc. Biol.* **19**, 170–177 (1999).
5. Bolton-Maggs, P. H. B. & Pasi, K. J. Haemophilias A and B. *Lancet* **361**, 1801–1809 (2003).
6. Toh, Y., Mizutani, A., Tokunaga, F., Muta, T. & Iwanaga, S. Morphology of the granular hemocytes of the Japanese horseshoe crab *Tachypleus tridentatus* and immunocytochemical localization of clotting factors and antimicrobial substances. *Cell Tissue Res.* **266**, 137–147 (1991).
7. Shibata, T., Kobayashi, Y., Ikeda, Y. & Kawabata, S.-I. Intermolecular autocatalytic activation of serine protease zymogen factor C through an active transition state responding to lipopolysaccharide. *J. Biol. Chem.* **293**, 11589–11599 (2018).
8. Kawabata, S.-i & Muta, T. Sadaaki Iwanaga: discovery of the lipopolysaccharide- and -1,3-d-glucan-mediated proteolytic cascade and unique proteins in invertebrate immunity. *J. Biochem.* **147**, 611–618 (2010).
9. Ashrafuzzaman, M. D. et al. Biomolecules of the horseshoe crab's hemolymph: components of an ancient defensive mechanism and its impact on the pharmaceutical and biomedical industry. *Cell. Microbiol.* **2022**, 1–17 (2022).
10. Hartwig, J. H. The platelet: form and function. *Semin. Hematol.* **43**, S94–S100 (2006).
11. van Geffen, J. P., Swieringa, F. & Heemskerk, J. W. M. Platelets and coagulation in thrombus formation: aberrations in the Scott syndrome. *Thromb. Res.* **141**, S12–S16 (2016).
12. Falati, S., Gross, P., Merrill-Skoloff, G., Furie, B. C. & Furie, B. Real-time in vivo imaging of platelets, tissue factor and fibrin during arterial thrombus formation in the mouse. *Nat. Med.* **8**, 1175–1180 (2002).
13. Furie, B. & Furie, B. C. Thrombus formation in vivo. *J. Clin. Investig.* **115**, 3355–3362 (2005).

14. Furie, B. & Furie, B. C. In vivo thrombus formation. *J. Thromb. Haemost.* **5**, 12–17 (2007).
15. Celi, A. et al. Thrombus formation: direct real-time observation and digital analysis of thrombus assembly in a living mouse by confocal and widefield intravital microscopy. *J. Thromb. Haemost.* **1**, 60–68 (2003).
16. Li, W., McIntyre, T. M. & Silverstein, R. L. Ferric chloride-induced murine carotid arterial injury: a model of redox pathology. *Redox Biol.* **1**, 50–55 (2013).
17. Denis, C. et al. A mouse model of severe von Willebrand disease: defects in hemostasis and thrombosis. *Proc. Natl Acad. Sci. USA***95**, 9524–9529 (1998).
18. Kuijpers, M. J. E. et al. Key role of platelet procoagulant activity in tissue factor-and collagen-dependent thrombus formation in arterioles and venules in vivo differential sensitivity to thrombin inhibition. *Microcirculation* **15**, 269–282 (2008).
19. Dubois, C., Panicot-Dubois, L., Gainor, J. F., Furie, B. C. & Furie, B. Thrombin-initiated platelet activation in vivo is vWF independent during thrombus formation in a laser injury model. *J. Clin. Investig.* **117**, 953–960 (2007).
20. Passam, F. H. et al. Both platelet- and endothelial cell-derived ERp5 support thrombus formation in a laser-induced mouse model of thrombosis. *Blood* **125**, 2276–2285 (2015).
21. Fukuoka, T., Hattori, K., Maruyama, H., Hirayama, M. & Tanahashi, N. Laser-induced thrombus formation in mouse brain microvasculature: effect of clopidogrel. *J. Thromb. Thrombolysis* **34**, 193–198 (2012).
22. Larsson, P. et al. Scanning laser-induced endothelial injury: a standardized and reproducible thrombosis model for intravital microscopy. *Sci. Rep.* **12**, 3955 (2022).
23. Rosen, E. D. et al. Laser-induced noninvasive vascular injury models in mice generate platelet- and coagulation-dependent thrombi. *Am. J. Pathol.* **158**, 1613–1622 (2001).
24. Barr, J. D., Chauhan, A. K., Schaeffer, G. V., Hansen, J. K. & Motto, D. G. Red blood cells mediate the onset of thrombosis in the ferric chloride murine model. *Blood* **121**, 3733–3741 (2013).
25. Getz, T. M. et al. Novel mouse hemostasis model for real-time determination of bleeding time and hemostatic plug composition. *J Thromb. Haemost.* **13**, 417–425 (2015).
26. Ballard-Kordeliski, A. et al. 4D intravital imaging studies identify platelets as the predominant cellular procoagulant surface in a mouse hemostasis model. *Blood* **144**, 1116–1126 (2024).
27. Sugita, S., Kato, M., Wataru, F. & Nakamura, M. Three-dimensional analysis of the thoracic aorta microscopic deformation during intraluminal pressurization. *Biomech. Model. Mechanobiol.* **19**, 147–157 (2020).
28. Zwaal, R. F. A., Comfurius, P. & Bevers, E. M. Scott syndrome, a bleeding disorder caused by defective scrambling of membrane phospholipids. *Biochim. Biophys. Acta (BBA)—Mol. Cell Biol. Lipids* **1636**, 119–128 (2004).
29. Sakurai, Y. et al. A microengineered vascularized bleeding model that integrates the principal components of hemostasis. *Nat. Commun.* **9**, 509 (2018).
30. Monroe, D. M., Hoffman, M. & Roberts, H. R. Transmission of a procoagulant signal from tissue factor-bearing cells to platelets. *Blood Coagul. Fibrinolysis* **7**, 459–464 (1996).
31. Campbell, R. A., Overmyer, K. A., Selzman, C. H., Sheridan, B. C. & Wolberg, A. S. Contributions of extravascular and intravascular cells to fibrin network formation, structure, and stability. *Blood* **114**, 4886–4896 (2009).
32. Maxwell, M. J. et al. Identification of a 2-stage platelet aggregation process mediating shear-dependent thrombus formation. *Blood* **109**, 566–576 (2007).
33. Ikeda, Y. et al. The role of von Willebrand factor and fibrinogen in platelet aggregation under varying shear stress. *J. Clin. Investig.* **87**, 1234–1240 (1991).
34. Kahn, M. L. et al. Protease-activated receptors 1 and 4 mediate activation of human platelets by thrombin. *J. Clin. Investig.* **103**, 879–887 (1999).
35. Nakanishi-Matsui, M. et al. PAR3 is a cofactor for PAR4 activation by thrombin. *Nature* **404**, 609–613 (2000).
36. Camerer, E., Huang, W. & Coughlin, S. R. Tissue factor- and factor X-dependent activation of protease-activated receptor 2 by factor VIIa. *Proc. Natl Acad. Sci. USA***97**, 5255–5260 (2000).
37. Sperry, J. L. et al. PAMPer Study Group. Prehospital plasma during air medical transport in trauma patients at risk for hemorrhagic shock. *N. Engl. J. Med.* **379**, 315–326 (2018).
38. Chapman, M. P. et al. Combat: initial experience with a randomized clinical trial of plasma-based resuscitation in the field for traumatic hemorrhagic shock. *Shock* **44**, 63–70 (2015).
39. Bi, L. et al. Targeted disruption of the mouse factor VIII gene produces a model of haemophilia A. *Nat. Genet.* **10**, 119–121 (1995).
40. Parry, G. C., Erlich, J. H., Carmeliet, P., Luther, T. & Mackman, N. Low levels of tissue factor are compatible with development and hemostasis in mice. *J. Clin. Investig.* **101**, 560–569 (1998).
41. Suzuki, J. et al. Calcium-dependent phospholipid scramblase activity of TMEM16 protein family members. *J. Biol. Chem.* **288**, 13305–13316 (2013).
42. Tiedt, R., Schomber, T., Hao-Shen, H. & Skoda, R. C. Pf4-Cre transgenic mice allow the generation of lineage-restricted gene knockouts for studying megakaryocyte and platelet function in vivo. *Blood* **109**, 1503–1506 (2007).
43. Nieswandt, B., Bergmeier, W., Rackebrandt, K., Gessner, J. E. & Zirngibl, H. Identification of critical antigen-specific mechanisms in the development of immune thrombocytopenic purpura in mice. *Blood* **96**, 2520–2527 (2000).

Acknowledgements

The Ano6 cKO mice used in this study were generated with permission obtained from S. Nagata (Osaka University, Japan). We would like to thank T. Ohmori (Jichi Medical University, Japan), M. Ishii (Osaka University, Japan) and S. Kawabata (Kyushu University, Japan) for useful discussions. We thank American Journal Experts (AJE) for English language editing and T. Kameoka, from Nikon Solutions Co., Ltd. for their technical assistance with microscopy.

Author contributions

Conceptualization: A.S.; Data curation: A.S., Naoki M., S.H., R.K., Y.N., and T.S.; Data interpretation: A.S., K.T., Naoki M., Nigel M., S.H., R.K., K.N., and M.S.; Formal analysis: A.S. and Naoki M.; Investigation: A.S.; Methodology: A.S.; Project administration: K.T., T.S., and M.S.; Resources: K.T., Nigel M., Y.N., and T.S.; Supervision: M.S.; Visualization: A.S.; Writing— original draft preparation: A.S. and Naoki M.; Writing—review and editing: A.S., Naoki M., K.T., Nigel M., S.H., R.K., Y.N., T.S., K.N., and M.S.

Competing interests

This study was funded by Chugai Pharmaceutical. The authors declare the following competing interests: A.S., K.T., Naoki M., S.H., R.K., Y.N., T.S., K.N., and M.S.: Members of the Medicinal Biology of Thrombosis and Haemostasis established by Nara Medical University and Chugai Pharmaceutical Co., Ltd. Naoki M., S.H., R.K., Y.N., and T.S.: Employees of Chugai Pharmaceutical Co., Ltd. Naoki M., S.H. and R.K.: Ownership of stock by Chugai Pharmaceutical Co., Ltd. M.S.: Patents for inventions related to products of Chugai Pharmaceutical Co., Ltd. K.T.: Grants or research support from the Japan Blood Products Organization, the Mother and Child Health Foundation and Novo Nordisk Pharma. M.S.: Takeda Pharmaceutical Co., Ltd., and CSL Behring; honoraria or consultation fees from Chugai Pharmaceutical Co., Ltd.; speaker bureau from Chugai Pharmaceutical Co., Ltd.; CSL Behring, Sanofi, Bayer, Novo Nordisk Pharma, Takeda Pharmaceutical Co., Ltd., Pfizer, and Fujimoto Seiyaku Corp. K.N.: Representative of Medicinal Biology of Thrombosis and

Haemostasis collaborative research laboratory; research support from Chugai Pharmaceutical Co., Ltd.; grants or research support from Chugai Pharmaceutical Co., Ltd.; Takeda Pharmaceutical Co., Ltd.; KM Biologics Co., Ltd.; Sanofi Co., Ltd.; Novo Nordisk Pharma Co., Ltd.; Bayer Co., Ltd.; AbbVie GK LLC; Janssen Pharmaceutical K.K. Co., Ltd.; honouraria or consultation fees from Chugai Pharmaceutical Co., Ltd.; Sanofi Co., Ltd.; and CSL Behring.

Additional information

Supplementary information The online version contains supplementary material available at https://doi.org/10.1038/s42003-025-07838-x.

Correspondence and requests for materials should be addressed to Asuka Sakata.

Peer review information *Communications Biology* thanks Eduardo Fuentes and the other, anonymous, reviewer(s) for their contribution to the peer review of this work. Primary Handling Editor: Christina Karlsson Rosenthal. A peer review file is available.